

Received May 6, 2020, accepted May 16, 2020, date of publication May 20, 2020, date of current version June 2, 2020.

Digital Object Identifier 10.1109/ACCESS.2020.2996022

Unsupervised Deep Learning CAD Scheme for the Detection of Malaria in Blood Smear Microscopic Images

PRIYADARSHINI ADYASHA PATTANAIK¹, MOHIT MITTAL², (Member, IEEE),
AND MOHAMMAD ZUBAIR KHAN³

¹Telecom SudParis, 91011 Évry, France

²Department of Information Science and Engineering, Kyoto Sangyo University, Kyoto 603-8555, Japan

³Department of Computer Science, College of Computer Science and Engineering, Taibah University, Madinah 41477, Saudi Arabia

Corresponding authors: Mohit Mittal (mohitmittal@ieee.org) and Mohammad Zubair Khan (mkhanb@taibahu.edu.sa)

ABSTRACT Recent advances in deep learning, coupled with the onslaught of unlabelled medical data have drawn ever-increasing research interests by discovering multiple levels of distributed representations and solving complex medical related problems. Malaria disease detection in early stage requires an accurate and precise diagnosis in order to achieve successful patient remission. This paper proposes a comprehensive computer-aided diagnosis (CAD) scheme for identifying the presence of malaria parasites in thick blood smear images. The parameters of the scheme are pre-trained by functional link artificial neural network followed by sparse stacked autoencoder. The optimum size of the CAD scheme used in this research is 12500-2500-100-50-2, where the input layer has 12500 nodes and Softmax classifier output layer has 2 nodes. Moreover, the 10- fold cross validation reflects that the classification is reliable and is applicable to new patient blood smear images. The proposed CAD scheme has been evaluated using malaria blood smear image data set, achieving a detection accuracy of 89.10%, a sensitivity of 93.90% and specificity of 83.10%. The extensive comparative experiment suggests that the proposed CAD scheme provides richer effectiveness and efficiency for malaria data set compared to other deep learning techniques for better diagnosis decision and management. This work implements a novel approach to fast processing and will be a beneficial tool in disease identification.

INDEX TERMS Computer-aided diagnosis (CAD), Deep learning, malaria parasite detection, microscopic blood smear images, digital pathology, K-fold cross-validation.

I. INTRODUCTION

Malaria is a deadly disease and major cause of infection worldwide. This epidemic disease has been recorded in every period of history due to its rapid demand and leading death rate. Malaria, is a fatal parasitic disease, with 212 million cases and 4,29,000 related death cases in 2015 are estimated worldwide. It is a life-threatening disease to pregnant women and children under five, as estimated around 3,03,000 children lost lives in 2015 [1]. Despite these statistics, the mortality rate due to malaria can be reduced by early fast and reliable diagnosis. The growth in malaria cases and unnatural geographical distribution are not stable because of various

The associate editor coordinating the review of this manuscript and approving it for publication was Marcin Woźniak^{id}.

reasons, like lack of highly trained expertise in rural areas, mismanagement of data, widespread of false and duplicate medicines, availability of low-cost diagnostic tools, global warming and much more [2]. This communicable disease is a complex rapidly growing disease and has become a challenge to handle due to the count of malaria parasites. Malaria detection is difficult and is too hard to differentiate parasite and non-parasite infected from the enormous density of blood smear microscopic images. The key to the accurate result of identification of infected parasites with minimum time, cost and effort is a challenge for the research expertizes. In this last few decades, the concept of visual inspection has emerged in the computer-aided diagnosis field, like a novel assistive software approach in clinical medical imaging and decision support. But, visual inspection of this global disease

is subjective, time-consuming and erroneous in nature. The visual procedure of characterizing and identifying of malaria parasite is one of the renowned fundamental problems to differentiate between stained blood smear microscopic image components. The traditional process of detecting malaria in the clinic is a manually tedious and time taking job with less chance of delivering an accurate result [2]. The increase in the number of malaria cases with the environment and the workload on a pathologist increases significantly, resulting in poor health-care services. Considering the above notable challenges, computer-aided diagnosis (CAD) has paved the way for better objective assessment for personalized health-care and diagnosis task. The development of CAD has successfully filled up the gap between the discriminative local appearances and the global image context with proper management of time series. The introduction of CAD may have a major impact on all subjects and imaging modalities by annotating imaging data sets and detecting abnormalities under a varying set of environmental conditions. The differences in size, shape and intensity variations in imaging protocol of cell components in blood smear microscopic images are some challenges faced by CAD [2]. However, the complexity of the malaria parasite detection through blood smear microscopic images and anisotropic voxel size with the large volume of unlabeled datasets generated by clinical procedures make the development of CAD model for malaria detection an exigent task in the vision community [3]–[5]. The limited availability of annotated malaria image data and large unlabelled static and dynamic samples is an extremely harder issue to handle [2]. Here, therefore the idea of Deep learning comes to light with record leading clever tricks on algorithms that can help to detect malaria parasites in an image no matter where they are located [3], [4], and [6]–[8].

The structure of this manuscript is systematically organized as follows. Section I introduces the concept of detection of malaria disease in blood microscopic image and CAD scheme. Section II briefly reviews the related works and the motivation. Section III promisingly discuss in detail the proposed CAD scheme step by step. Section IV defines the data set collection and methodology. Section V represents the experiments and results based on comparative performance of proposed model with other estimated deep learning techniques. Section VI presents concluding remarks of this paper.

II. RELATED WORK AND OUR MOTIVATION

In recent years, several artificial neural networks with multiple layers have been proposed for a variety of health diagnosis using microscopic images, however, Razzak *et al.* [3] proposed a powerful model named Deep learning in 2006 which again brought the concept from 1989. Deep learning is a broad family and a subfield of machine learning with hierarchical learning deep image architecture which learns high-level features from the given pixel intensities. Deep learning techniques have many success stories for CAD tasks because they solve many tedious problems reducing the task of new

parameters that they can calculate an accurate output parameter [3]. The deep neural network (DNN) architecture carries many multiple hidden layers and so the network is called deep, not only in classification tasks but also in regression. DNN is an emerging approach to excellent performance in various variants, such as dimensionality reduction, object segmentation, modeling textures, modeling motion, information retrieval, robotics, natural language processing, collaborative filtering, so on. Shen *et al.* [5] used Convolutional neural network (CNN) as medical image classifier in order to address two specific CAD problems, like thoracoabdominal lymph node (LN) estimation and interstitial lung disease (ILD) classification. The overall CNN model analysis and extensive empirical evaluation help to design high performance with good accuracy CAD model for medical image tasks. Many CAD studies focused on monitoring the prognosis and direct differentiation of malaria parasites and non-parasites [3], [8], [9]. Das *et al.* [6] used SVM and Naive Bayes machine learning classifier to achieve accuracies of 84% and 83.5% for building automated diagnostic system for malaria detection. Ross *et al.* [4] designed a three-layer neural network as a classifier for automated malaria diagnosis on thin blood smears at an accuracy of 85%. Li and Orchard [10] proposed an Edge Directed Predictor (EDP) in order to structure an improvised detection model using Least Square based adaptation. Besides this popular method, there is a huge range of lossless compression techniques that are fully mathematical optimized frameworks for different [7] and [11]–[13] overviewed a comprehensive comparison of feature selection based machine learning algorithms for automated optimization of malarial cell recognition in detail. These machine learning methods yet need good improvisation for feature extraction because it still requires trained skilled experts to handle data and smart techniques for calculating the prognosis of the disease [13]. Furthermore, recent observations have revealed that the accedence rates among the researchers and pathologists for the identification of this plague have alarmingly decreased [14]. Referring to the above concern, some faced challenges can be summarized together to build a new CAD scheme.

ANN architectures based CAD schemes consist of many levels and layers of non-linearities complex mappings. The layerwise network of multiple hidden layers creates a complex environment with gradient-based optimization getting stuck in poor outputs [15]. To overcome this bottleneck situation, a greedy layer-wise training method by unsupervised pretraining and back-propagating one layer at a time is applied. The better representation of high dimensional data to low-dimensional encoding space is done by the unsupervised pre-training phase of each layer resulting in poor local optima to more sparse feature learning. The deep belief network (DBN) addressed by Arel *et al.* [15] carries an advantage of the systematic layer by layer greedy learning strategy, and fine tuning all of the weights together with the crave output. Nair and Hinton [16] introduced a modified two-layer DBN where the first layer learns local, oriented,

edge filters and the next layer comprises of a variety of contour corners and junctions, aiming to form a robust model. Nigam *et al.* [17] constructed a deep energy model (DEM) of a single level of stochastic hidden layers for effective qualitative and quantitative improvements done using Hybrid Monte Carlo (HMC) over greedy layer-wise training. Dahl *et al.* [18] proposed a new DNN that combines DBN with a Mean-Covariance RBM for feature extraction and addresses the inefficiency in terms of this limitations of phone recognition. Phone recognition helps to detect who is speaking in the phone. Liou *et al.* [19] defined a proper special type of autoencoder approach for learning efficient encodings to remove the problem of getting stuck in local optima is to pre-train the network layers with initial updated weights. A neural network comprises of the high dimension of features, resulting in the issue of overfitting. The multiple layers in ANN, result in low performance and mismanagement of update weights, which leads the whole network prone to overfitting [20]. To solve it, a common way is the introduction of dropout method and use of equal weights for all parameters by supervised training. The concept of dropout was proposed by [21] and demonstrated in depth by [22]. Dropout is an extremely functional ensemble learning which further improved by [20] and [23]. Thompson *et al.* [24] added a Spatial drop out layer to the existing CNN model of Mann *et al.* [25] to improve the precision of the spatial localization accuracy and reuse the hidden layer convolution features. In order, to make the learning space more stable and robust, many researchers [26], [27] have depicted many variations of autoencoder making the various classes more separable. Masci *et al.* [28] defined a convolutional autoencoder for hierarchical feature representation to preserve spatial locality using dropout method efficiently. Hu *et al.* [29] measured a deep autoencoder combined with a softmax classifier to detect Alzheimer's disease from MRI image data sets. This approach shows that the proposed method works well as compared to other traditional handcrafted methods. Shan and Li [30] introduced a stacked sparse autoencoder for learning high-dimensional microaneurysms detection from fundus images. Thus, we can say that the deep learning method outperforms classical CAD architectures, largely due to the noise tolerance and dominated medical image applications. Autoencoder with drop out is called as Denoising Autoencoder (Noise tolerance), deterministic deep learning approach, has a high level compressed representation of input distinguish features automatically based on pixel intensities. Chen *et al.* [31] modeled a new type of CAD framework that can outline pulmonary nodules with different annotated degrees of the 9 semantic features. Vincent *et al.* [32] proposed a denoising autoencoder (DAE) model to recover the exact input from a suborn version. The designed model reconstructs each image pixel from the corresponding dense and noisy background region. Rifai *et al.* [33] proposed contractive autoencoder motivated with learning robust representations followed by adding an advantage to the reconstruction error function. Both DAE and CAE work successfully well

in the Unsupervised and Transfer Learning Challenge [33]. Zhang *et al.* [34] and Asl *et al.* [35] demonstrated apart based deep learning representation using sparse auto-encoders to gain high reconstructed quality decompose data as compared with the traditional autoencoder. It also demonstrates how to get a useful representation from data that perceive the hidden layer of high-dimensional human brain data based on autoencoders. Sparse autoencoders have various potential advantages just like SVM, the high-dimensional enhances the likelihood that various stages will be easily separable. Sparse autoencoder framework interprets the whole structure into a number of parts for better representations; biomedical researchers gain interest in using sparse auto-encoders due to its best results in biological vision areas. Another challenge is the process of saliency estimation of weighting features. Shen and Wu [36] utilized the mid-level and high-level parameters gathered from salient regions to represented a multi-layer network with a linear SVM [37] highlighting the clear visible semantic feature objects. To overcome the problem of saliency estimation detection, [38] computed the central patch with its neighboring patches using sparse reconstruction deep networks. To pop out the challenge of salient detection, many computational models have been proposed using traditional parameters like intensity, color, gist [39], integration theory [40], orientation [41], symmetry [42], and local steering kernel [43] for estimating saliency. Zhao *et al.* [44] presented a comprehensive survey on different learning based salient estimation algorithms which can be useful to many computer-aided diagnosis researchers. Although the learning based salient detection techniques provide an outstanding performance, but maximum of them are fully dependent on labeled trained datasets. Unfortunately, a gap gets created due to unavailability of the costly tools and poor management of data resulting in a key problem between data and saliency. DNN has emerged as specific object categories, and lead to many success stories in a wide variety of tasks [38] and [45]–[49]. To address this challenge, CNN has been used with remarkable results for determining the contribution of weight features along with the increasing interest of the expansion of feature dimension by Li and Yu *et al.* [50].

The popularity and recent success of supervised learning have obscured unsupervised learning in many fields. DNN model like Restricted Boltzmann Machine (RBM) and Autoencoder (AE) have emerged from pixel level information processing to the patch based comparison, the prediction quality is greatly improved. AE, a fully connected framework which aims in lower reconstruction error at each layer, delivers a better initialization of layer parameters. This learning algorithm imposes a limitation on parameters with a compressed representation of encoder and decoder representation [51]. In medical field of diagnosis, the AE represents the ability of the proposed model to predict the probability of disease treatment for a patient. This early prediction in health care could be directly proportional to saving patients lives. The first stage of AE model is compression and feature extraction of selective statistical or geometric features in medical data

to achieve the best low dimensional vector. The second stage of compression leads to the decoder stage where the task is to reconstruct an identical version of the input image by going through many operations. This feedforward neural network inspires globally through its data reconstruction ability and robustness against noise measurement (Sparse autoencoder) [52]. The introduction of part-based representation by Asl *et al.* [35] demonstrates a meaningful data representation for improving the ability to untwine the hidden layers and levels of unlabelled data in the human brain using deep autoencoders. The prediction performance of the proposed DNN method [35] gives a better result as compared to other techniques. The whole workflow is done on the MNIST dataset, ORL data set, NORB dataset and REUTERS-21578 text data set. The hierarchical layers of visual cortex data structured by part based decomposition give an expensive fast improved DNN of optimization. As a result, the new CAD method is a quite challenging approach for quantitative image diagnosis and classification.

In this paper, a novel alternate work has been done harmoniously using Functional Link Artificial Neural Network (FLANN) and Stacked Sparse Autoencoder (SSAE) techniques for malaria parasite detection. This proposed work binds an original SSAE with the FLANN based on trigonometric polynomials introducing an unsupervised information, to achieve a meaningful detection from high dimensional data. Inspired by the dimensionality reduction detection approaches and successful application of DNN, we have designed a multi-objective architecture to explore a new novel computationally CAD scheme offering an unprecedented power and efficiency automatically. This CAD scheme offers a promising strategy to investigate the malaria infection and a tool to handle large image dataset with less reconstruction error. In this study, we have bound the FLANN in the first section with the SSAE followed by a Softmax Classifier, which introduces unsupervised data, to make use of the unlabelled images well. Finally, the low dimensional, high-level parameters were eventually fed into a Softmax Classifier (SMC) for categorizing malaria parasites from non-parasites within an independent testing set. The proposed CAD scheme is a deep learning architecture established for simultaneous feature extraction and classification with drastically less computational complexity.

The major contributions of this proposed deep learning CAD scheme can be summarized in three folds. FLANN, which is the first stage of CAD scheme, is the process of the single layer structure and is used for the nonlinear dynamic system, determining whether the thick blood smear microscopic image is malarial infected or non-infected using the popular back-propagation algorithm. The back propagation algorithm uses the method of gradient descent with multi-layer perceptrons and sigmoidal nonlinearities for minimizing the error function in the weight space. The back propagation algorithm improves its convergence process along with the recognized patterns superiorly. Using FLANN enables faster convergence rate and less computational load

than other traditional neural network methods [53]. The first stage includes the functional expansion of the input information with no hidden layers, resulting in a simple network of identification of complex nonlinear functions. This way of expansion helps in providing greater discrimination capability in the input space and learning becomes faster. Finding the proper correct preprocessing, normalization or change of input data can be challenging before the training process. So, the introduction of FLANN in this CAD scheme acts as a preprocessing savior to select an optimal set of hyperparameters for the significant training process. The second contribution lies in the novelty of SSAE model which is able to impose a limitation on features (dimension, hidden layers), further discovering the latent structure of data in a high dimensional space [54]. The proper pre-training of each layer initialization in autoencoder helps in better representation and overcoming vanishing gradient-based optimization problem. The autoencoder is a deterministic feed-forward neural network which improves the CAD scheme prediction performance with better layer-wise initialization computing saliency [55]. Third, a Softmax classifier (SMC) [56] is added to effectively differentiate malaria-infected and non-infected blood smear microscopic images. As the autoencoder learning process is unsupervised, the model accepts high-level data as input and reconstructs an output that is similar to the input. This reconstructed output maps between the input and the class labels fed to the supervised model of SMC produces a practical solution of value 0 and 1, that can be interpreted as malaria-infected or non-infected thick blood smear microscopic image. As a result, the weights of the entire CAD scheme are trained referring to fine tuning, producing an effective model for malaria parasite monitoring [57], [58].

To sum up the entire work, training of the CAD scheme framework is done to plot a learning model automatically processing the high-level features associated with parasite detection in malaria diagnosis. Our approach aims to execute an accurate and robust machine learning model and is compared with some neuron crafted features like original Auto-encoder (AE), Stacked Auto-encoder (SAE) and Restricted Boltzmann Machine (RBM) in terms of accuracy of performance on blood smear microscopic images datasets.

III. PROPOSED CAD SCHEME

In this section, we reinforced a trained model using FLANN and SSAE for malaria parasite detection in thick blood smear microscopic images. For malaria parasite detection, we trained a CAD model to differentiate the malaria parasites from the normal blood components. The CAD scheme is a neural network consisting of multiple layers of FLANN and SSAE as seen from Figure 1 learning models, in which the output parameters of each layer are wired to the input and are trained layer by layer. This scheme network can be used not only for dimensionality reduction but also for decreasing the computational complexity. This model is mainly focused on two phases of learning for better malaria parasite detection in blood smear microscopic images. In this

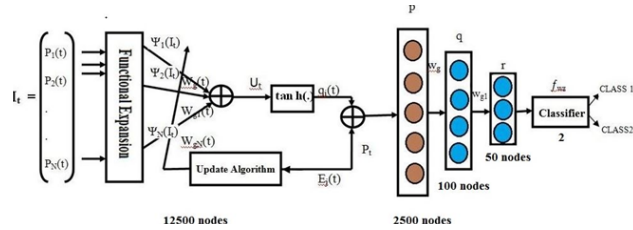


FIGURE 1. Structure of a proposed computer-aided diagnostic CAD scheme.

model, we use thick blood smear microscopic images, which is 20-40 times more fragile than thin blood smear microscopic for screening malaria parasites, with a detection limit of 10-50 trophozoites/ μL [59]. To extract the image features, the thick blood smear was stained using Field stain at $\times 1000$ magnification followed by segmenting the stained objects using level set method [60]. In this study, we illustrate the training of 2 stage of Chebyshev FLANN [53] and the usage of the subsequent SSAE [54] for the feature extraction of stained objects through a classification using Softmax.

A. EXPANSION OF INPUT DATA

The first-stage learning functional approximation is a single layer model consisting of one input and one output layer based on trigonometric expansion. Using the functionally expanded features, FLANN overcomes the high computational complexity of the nonlinear problems. The single layer FLANN is easy to train and effectively increases the dimensionality of the input parameters providing a broad discrimination capability on the input pattern space. The first stage of expansion of input data of CAD algorithm is shown below,

Step 1: Initialize a training pattern by $\{I_t, J_t\}$ and weight matrix by $W_{g1}(t)$. The discrete-time index t is given by $t = t + \lambda T$ for $t = 1, 2, 3, \dots T$ and $\lambda = 0, 1, 2, 3 \dots T$, where T is the total number of training patterns.

Step 2: As t^{th} an instant, the n -dimensional input pattern and the m -dimensional FLANN output are given by $[I_t = p_1(t), p_2(t), \dots p_n(t)]^U$ respectively. Its corresponding target pattern is represented by $[J_t = q_1(t), q_2(t), \dots q_m(t)]^U$.

Step3: The dimension of the input pattern increases from n to N by a basis function ψ given by $\psi(I_t) = [\psi_1(I_t), \psi_2(I_t) \dots \psi_N(I_t)]^U$.

Step 4: The $(m \times N)$ -dimensional weight is given by $W_g(t) = [W_{g1}(t), W_{g2}(t) \dots W_{gm}(t)]^U$ where $W_{gj}(t)$ is the weight vector associated with j^{th} output and is given by $W_{gj}(t) = [v_{j1}(t), v_{j2}(t) \dots v_{jN}(t)]$. The j^{th} output nonlinear function is formed by multiplying with a set of random initialized weights applied with patterns summed to produce estimated output. The j^{th} output of the FLANN is given by,

$$\hat{q}_j(t) = \rho\left(\sum_{i=1}^N v_{j1}(t)\psi_i(I_t)\right) = \rho(I_j(t)\psi(I_t)) \quad (1)$$

for $j = 1, 2, 3 \dots m$

Step 5: The error associated with j^{th} output node is given by $E(t) = q_j(t) - \hat{q}_j(t)$

Step 6: Using the BP algorithm, weights of the FLANN can be updated as,

$$W_g(t + 1) = [W_g(t) + \mu \Delta(t) + \gamma \Delta(t - 1)] \quad (2)$$

$$\Delta(t) = \delta(t)[\psi(I_t)]^U \quad (3)$$

where,

$\delta(t) = [\delta_1(t)\delta_2(t)\delta_m(t)]^U$, $\delta_j(t) = (1 - \hat{q}_j^2(t))E_j(t)$, μ and γ are learning

B. COMPRESSION OF INPUT DATA

The output of the functional expansion gets into the stacked sparse autoencoder as an input with two hidden layer feature representation in the second stage.

Step 7: The $q_j(t)$ is the output of the learning algorithm gets adjusted and goes p_t as pt as input, where the $p \in [0, 1]^d$ input vector and the hidden representation is $q \in [0, 1]^d$.

$$q = f_\theta(p) = S_g(W_g p + B) \quad (4)$$

with $\theta = \{W_g, B\}$

$$S_g(p) = \frac{1}{1 + e^{-p}} \quad (5)$$

$$r = h_{\theta'}(q) = S_g(W_{g1} q + B') \quad (6)$$

with $\theta' = \{W_{g1}, B'\}$

Step 8: $p^{(i)}$ is mapping to the corresponding $q^{(i)}$. The basic idea here is to construct the mapping $p^{(i)} \rightarrow q^{(i)}$ reflects essential structure with the reconstruction of $p^{(i)}$ and $r^{(i)}$.

Step 9: Weight matrix W_{g1} may optionally be constrained by $W_g = W_g^T$.

$$r^{(i)} \approx p^{(i)} \quad (7)$$

$$p^{(i)} \rightarrow q^{(i)} \quad (8)$$

Step 10: θ and θ' of the second stage of the CAD scheme are optimized to minimize the avg. reconstruction error.

$$\begin{aligned} (\theta^*, \theta'^* &= \arg_{\theta, \theta'} \min \frac{1}{n} \sum_{i=1}^n L_S(p^{(i)}, q^{(i)}) \\ &\arg_{\theta, \theta'} \min \frac{1}{n} \sum_{i=1}^n L_S(p^{(i)}, h_{\theta'}(p^{(i)})) \end{aligned} \quad (9)$$

Step 11: Encoder f and decoder h

$$f : I \rightarrow A \quad (10)$$

$$h : A \rightarrow I' \quad (11)$$

$$A = \zeta_1(W_g p + B) \quad (12)$$

$$p' = \zeta_2(W_{g1} A + B') \quad (13)$$

ζ is an element-wise activation function such as sigmoid or rule.

Step 12: The second stage of the model can be trained to minimize reconstruction error (such as sum of squared errors)

$$L_S(p, p') = \|p - p'\|^2 = \|p - \zeta_2(W_{g1}(\zeta_1(W_g p + B)) + B')\|^2 \quad (14)$$

C. CLASSIFICATION

Step 13: The third stage of the whole CAD scheme involves Softmax Classifier which generalizes the logistic regression as

$$f_{W_g^{(3)}} = \frac{1}{1 + \exp(W_g^{(3)T} r)} \tag{15}$$

where $f_{W_g^{(3)}}$ represents the sigmoid function with $W^{(3)}$ parameters. The input r of the classifier is a high-level representation of nuclear structures with $W^{(3)}$ parameters. By studying the overall CAD scheme with $W^{(3)}$ via accuracy and detection time is recorded.

Step 14: Considering, the whole model the total error associated with the CAD scheme is given by

$$E = E_j(t) + L_s(p, p') \tag{16}$$

IV. DATA COLLECTION AND METHODOLOGY

A. DATASET

A set of 1182 Field-stained malaria-infected blood smear microscopic images are obtained from Android smartphone to a Brunel SP150 microscope by a group of data scientists from the AI research group at Makerere University, as part of the collaborative research on automated malaria infection diagnosis. The blood cell images are RGB color images with a 750×750 pixel resolution [59]. The Field-stained malaria blood smear slides are scanned and captured into 3D-printed phone adapters, at $1000\times$ optical magnification.

B. OTHER COMPARATIVE DEEP LEARNING BASED MODELS

1) AE + SMC BASED MALARIA PARASITE DETECTION METHOD

The original autoencoder is a single layer feedforward network of deterministic approach consisting of an input layer, one hidden layer, and an output layer. The input and hidden layer together form the encoder part and the hidden layer and output layer combines to form a decoder part, as shown in Figure 2. The hidden layer is smaller in size than the input layer, as the autoencoder compresses the information and focuses on useful extracted features for the effective performance of the model [54].

2) SAE + SMC BASED MALARIA PARASITE DETECTION METHOD

In this model, the input feature learned of SMC classifier via the use of two hidden layers of stack autoencoder from an input malaria blood smear microscopic image [54]. In the SAE + SMC network architecture (Figure. 3), the features extracted by SAE are feed as input to SMC [54] for classifying the infected and non-infected malaria.

3) TAE + SMC BASED MALARIA PARASITE DETECTION METHOD

Three-layer Sparse Autoencoder (TAE) is three hidden layers based autoencoder which is also known as deeply stacked

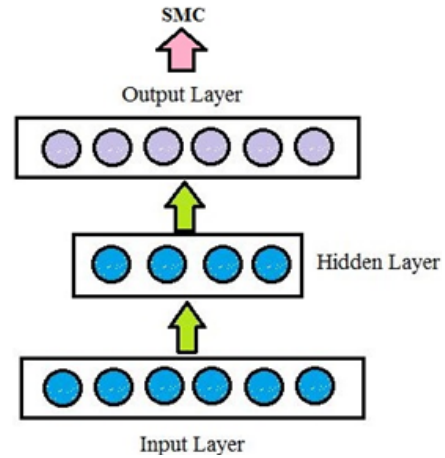


FIGURE 2. Basic autoencoder (AE) plus softmax (SMC) architecture.

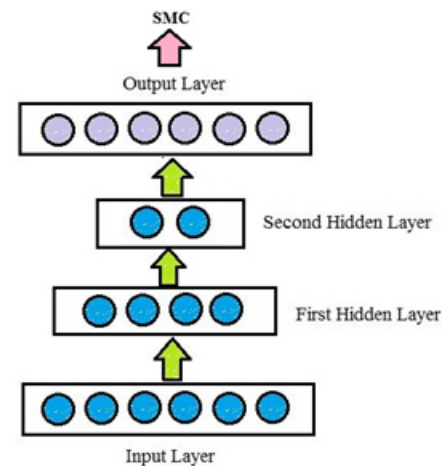


FIGURE 3. 2 layers sparse autoencoder (SAE) + softmax (SMC) architecture.

autoencoder [54]. In order to handle high dimension input data, a single hidden layer of original autoencoder may not be suitable, therefore stacked based deep third autoencoder is used as shown in Figure 4.

4) RBM + SMC BASED MALARIA PARASITE DETECTION METHOD

Restricted Boltzmann Machine (RBM) is a variant of the stochastic recurrent neural network. It is a probability distribution ‘P’ of observed input data (visible units) as the primary layer and the second layer consists of latent variables (hidden units). The observed input data units and hidden units together are associated with symmetric weights, and the visible and hidden units are pointed by bias weights [61]. RBM is used for fine-tuning the deep neural network with minimum reconstruction error (Figure 5). For each example, let’s define, ‘V’ is the visible units and ‘H’ is the hidden unit which together is restricted to form a bipartite graph allowing implementation of more efficient training algorithms.

$$(P(HV_1) = P(H_1 V_1)P(H_2 V_1) \dots P(H_n V_1))$$

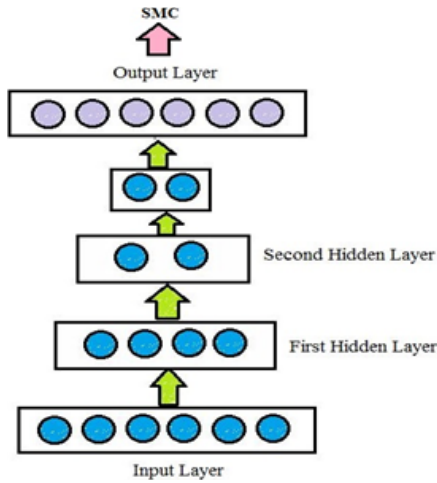


FIGURE 4. 3 layers sparse autoencoder (TAE) + softmax (SMC) architecture.

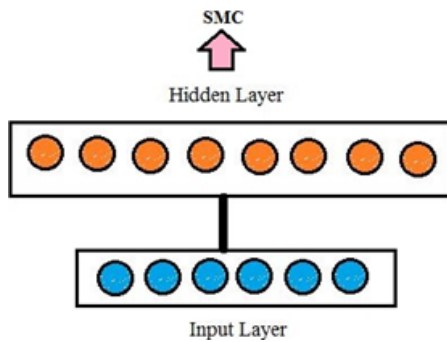


FIGURE 5. RBM plus Softmax (SMC) architecture.

The energy function of the model is given by [5].

$$\begin{aligned}
 (E(V, H, \theta)) = & - \sum_{m=1}^v \sum_{n=1}^H W_{mn} V_m H_n \\
 & - \sum_{m=1}^v B_m V_m - \sum_{n=1}^H A_n H_n
 \end{aligned}$$

where $\theta = \{W, B, A\}$ is the model parameter, A_{mn} and B_{mn} are the biases of the hidden and visible units, respectively.

C. EVALUATION METRICS

For performance evaluation, we have considered three evaluation metrics namely:

- 1) K-Fold cross-validation: The proposed CAD scheme performance is validated using K-Fold cross-validation.
- 2) Class Performance: Effectiveness of the proposed model is measured in terms of mean square error level and ROC curve.
- 3) Baselines for Comparisons: The proposed CAD scheme is compared with well-known deep learning techniques in terms of accuracy and detection time.

V. EXPERIMENTS AND RESULTS

A. COMPUTATIONAL CONSIDERATION

Our experiments carried out on a server with Intel Core i5 CPU with 16 GB of RAM with software implementation being performed using MATLAB 2016 b. The size of

each normalized image was 50×50 pixels perfect square. The proposed CAD scheme is compared against four other benchmarked deep learning based algorithms for computational efficiency under a similar environment of computational consideration. In terms of detection time and accuracy, the proposed CAD scheme was actually more efficient compared to the four other benchmarked deep learning-based algorithms.

B. K-FOLD CROSS VALIDATION

The malaria images are split using K-Fold cross-validation into two subgroups for K subset as testing and the other is K-1 subsets as training. This way of randomly dividing the data set is otherwise named as K rotation estimation. The goal of this validation is to use each data point in order to test the set exactly once and then train the set K-1 times to reduce the problem of over-fitting. Figure 6. reports the performance gradient on detection and classification on a 10-fold cross-validation.

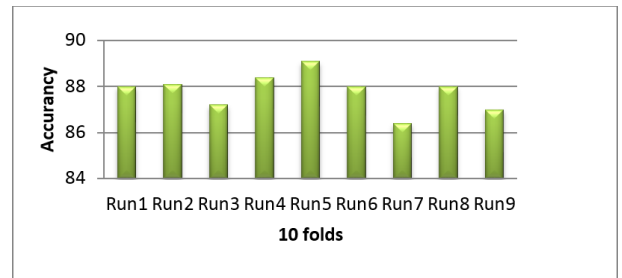


FIGURE 6. Graph for performance of the proposed CAD scheme.

At each time, nine-fold is considered for training and the left portion for testing. We perform 10 fold cross validation repeatedly for statistical analysis and to overcome the problem of over-fitting. Here, the classification performance of our proposed CAD scheme over 10 runs of 10- fold cross validation is represented in Figure 6. The 10 fold cross validation presents an evaluation study of results using statistical metrics via sensitivity, specificity, accuracy and detection time to note the effectiveness of the proposed scheme. The experiment presents the performance across each fold. In Figure 6. we observe that the CAD scheme provides the highest accuracy in fold 4-6, while is lower only in fold 7 which has an imbalance in the distribution of subcategories of infected and non-infected cases. The output results obtained from the proposed scheme indicated that the extracted features were informative. The k value decreases in fold 3 and fold 7, due to the instability of the training sets and smaller sample sizes. In this situation, we mainly focus on folds with better distribution of training and testing sets and repeat runs for a better approach.

C. CLASS PERFORMANCE

The remarkable quantitative performance of the CAD scheme and its comparison with different models is seen from

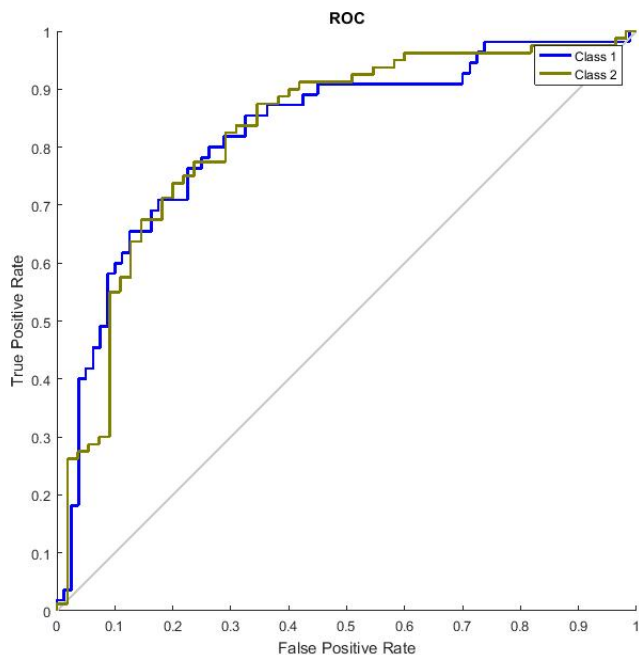


FIGURE 7. ROC curve on the malaria dataset using the proposed CAD scheme representing the noninfected blood smear as Class1 and infected as Class2.

Table 1 and is analyzed using True Positive, False Positive and Accuracy metrics. These quantitative volumetric measures are widely utilized in several studies [62]. The ultimate goal of any novel CAD scheme for a deep learning method is to achieve better generalization performance. In this paper, the correct detection of malaria parasites of blood smear microscopic images TP (true positives) was identified and FP, FN refers as false positive rate and the false negative rate is identified, respectively. After computing the TP, FP, FN and the absolute errors, the performance of the proposed CAD scheme is represented in an area under the receiver operating characteristic (ROC) curve and performance gradient in Figure 7 and Figure 8 respectively.

TABLE 1. Accuracies of broadly used deep learning techniques and the proposed method for AE + SMC, SAE + SMC, TAE + SMC, RBM, and proposed CAD scheme.

Deep Learning Techniques	Accuracy(%)
AE+ SMC	78.20
SAE+ SMC	80.70
TAE+ SMC	85.89
RBM	82.50
Proposed CAD Scheme	89.10

In this paper, it is experimentally demonstrated for the malaria blood smear microscopic image data set, where class I achieves infected and class II as non-infected represented in the ROC curve in Figure 7. In order to overcome the Intra expert and inter-expert variability and reduce the burden of clinical experts for identifying malaria parasite in microscopic images, it is desirable to use an automatic CAD scheme.

D. BASELINES FOR COMPARISONS

In order to discuss the effectiveness of our proposed CAD model, the model is compared against four other deep learning models [54] as shown in Table 1. for identifying malaria blood smear microscopic images from the dataset.

The proposed CAD network architecture has successfully achieved an accuracy of 89.10 % on the test set using a Softmax classifier in the malaria parasite detection task. The performance analysis of the trained CAD scheme is evaluated in comparison to several popular deep learning algorithms as given in Table 1. The comparison shows CAD scheme can detect the malaria-infected parasite microscopic images more efficiently without removing important features. The results in Table 1 and Table 2 toes the mark with other researchers. Patra *et al.* [38] found FLANN algorithm as the most suitable pre-processing savior to select an optimal set of hyperparameters for the significant result. It requires less computational time and works superior to that of Multilayer preceptor. Madabhushi *et al.* [54] proved SSAE gives better performance in automated nuclei detection of breast cancer histopathology than other beach marked deep learning algorithms. Considering the reviews, it confirms the effectiveness of the CAD scheme.

TABLE 2. The execution time of AE + SMC, SAE + SMC, TAE + SMC, RBM, and proposed CAD scheme when evaluated on test image of dimensions 750 × 750 pixels.

Deep Learning Techniques	Detection Time (in minutes)
AE+ SMC	00:08:43
SAE+ SMC	00:12:06
TAE+ SMC	00:14:28
RBM	00:12:15
Proposed CAD Scheme	00:03:24

In Table 1, AE + SMC based malaria parasite detection method is one of the most widely used deep learning method which puts an accuracy of 78.20% in thick malaria blood smear microscopic image data set, with a specificity of 87.67% and sensitivity of 67.89%. SAE + SMC is a two hidden layered based deep learning technique providing an accuracy of 80.70% with a specificity of 79.50% and sensitivity of 81.90%. TAE + SMC method delivers an accuracy of 85.89% and 87.88% of specificity. The other deep learning technique named RBM provides an accuracy of 82.50%, a sensitivity measure of 78.60% and specificity of 85.20%. It can be noted that there is a significant difference in order of the statistical metrics between the proposed scheme and deep learning based benchmarked algorithms. The Table 2 illustrates, the malaria parasite detection time for each of these deep learning techniques. The detection time is the time needed to finish all tasks in the workflow of the CAD scheme, making easier detection and less time-consuming.

In this paper, we have shown an extensive comparison of several deep learning techniques with promising results of the proposed CAD scheme on classifying infected and non-infected malaria parasite classes. CAD scheme is a powerful tool for image analysis and malaria disease detection because

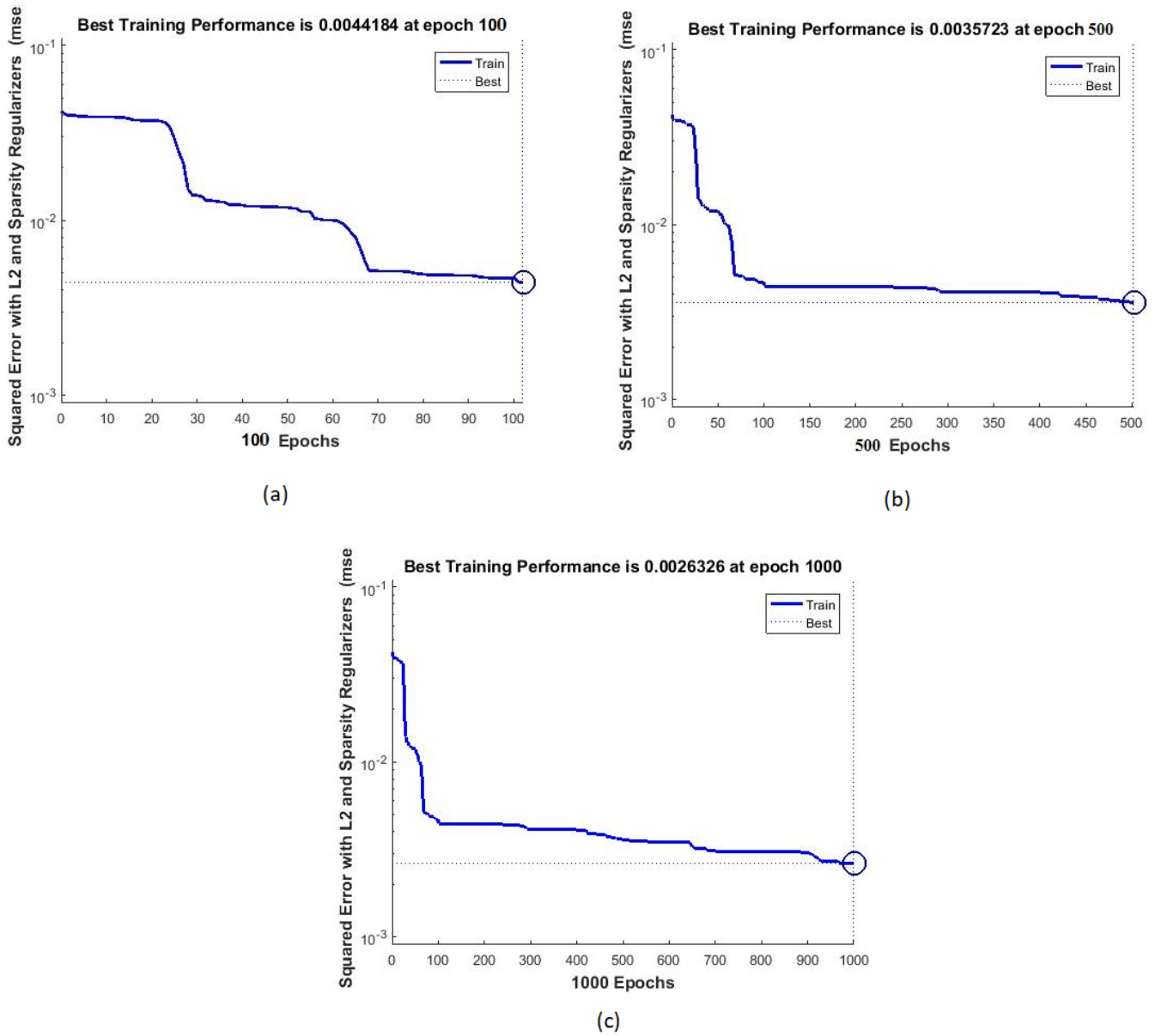


FIGURE 8. Performance evaluation of bandwidth and no. of epochs to achieve mean square error level at a different no. of epochs of CAD scheme.

it makes strong and correct adjustments as per specific task, leading to improving performance. From the Table 1, it is tangible that the proposed CAD scheme outperforms the other existing deep learning techniques in terms of accuracy. The proposed CAD scheme has attained an F-measure of 94.50% with a sensitivity of 93.90% and specificity of 83.10%. However, the computational complexity of the entire CAD scheme architecture remains balance as the number of layers and nodes in each layer increase. The proposed scheme leads to faster learning and less computational load as seen from Table 2 with better representation and overcomes various problems like gradient-based optimization, overfitting, and salient estimation of weighting features, to some extent. The proposed model takes the least detection time of 3 minutes 24 seconds than other benchmark deep learning techniques in

identifying malaria. The CAD scheme can capture high-level representations of pixel intensity in an unsupervised manner enabling the SMC classifier to work effectively for detecting malaria infected images from blood smear microscopic images.

VI. CONCLUSION

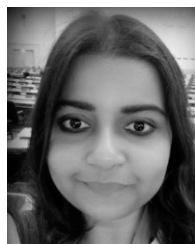
This paper addresses a novel comprehensive computer-aided diagnosis (CAD) scheme using deep learning network to identify the presence of malaria parasites in thick blood smear microscopic images. The work implements a novel approach to fast processing and delivers better results in terms of accuracy and detection time using microscopic thick blood smear images. Moreover, the 10- fold cross validation reflects that the classification is reliable and is applicable to new

patient blood smear microscopic images. Further, we found that the CAD scheme performs much better than broadly used deep learning techniques using the same dataset. Our experimental results show that the CAD scheme has overcome the faced challenges to a larger extent as summarized in this paper and has effectively identified the infected malaria parasites in thick blood smear microscopic images with an accuracy of 89.10% and execution time of 3 minutes 24 seconds. For better analysis and deeper classification of blood smear images, we aim to evolve a novel simplified deep learning model for classifying the different types of malaria plasmodium.

REFERENCES

- [1] C. Boschi-Pinto, T. R. Dilip, and A. Costello, "Association between community management of pneumonia and diarrhoea in high-burden countries and the decline in under-five mortality rates: An ecological analysis," *BMJ Open*, vol. 7, no. 2, Feb. 2017, Art. no. e012639.
- [2] L. Rosado, J. M. Correia da Costa, D. Elias, and J. S. Cardoso, "A review of automatic malaria parasites detection and segmentation in microscopic images," *Anti-Infective Agents*, vol. 14, no. 1, pp. 11–22, Mar. 2016.
- [3] M. I. Razzak, S. Naz, and A. Zaib, "Deep learning for medical image processing: Overview, challenges and the future," in *Classification in BioApps* (Lecture Notes in Computational Vision and Biomechanics), vol. 26. 2018.
- [4] N. E. Ross, C. J. Pritchard, D. M. Rubin, and A. G. Dusé, "Automated image processing method for the diagnosis and classification of malaria on thin blood smears," *Med. Biol. Eng. Comput.*, vol. 44, no. 5, pp. 427–436, May 2006.
- [5] H. Shen, W. David Pan, Y. Dong, and M. Alim, "Lossless compression of curated erythrocyte images using deep autoencoders for malaria infection diagnosis," in *Proc. Picture Coding Symp. (PCS)*, 2016, pp. 1–5.
- [6] D. K. Das, R. Mukherjee, and C. Chakraborty, "Computational microscopic imaging for malaria parasite detection: A systematic review," *J. Microsc.*, vol. 260, no. 1, pp. 1–19, Oct. 2015.
- [7] L. Itti, "Automatic foveation for video compression using a neurobiological model of visual attention," *IEEE Trans. Image Process.*, vol. 13, no. 10, pp. 1304–1318, Oct. 2004.
- [8] F. B. Tek, A. G. Dempster, and Á. Kale, "Parasite detection and identification for automated thin blood film malaria diagnosis," *Comput. Vis. Image Understand.*, vol. 114, no. 1, pp. 21–32, Jan. 2010.
- [9] S. Raviraja, G. Bajpai, and S. K. Sharma, "Analysis of detecting the malarial parasite infected blood images using statistical based approach," in *Proc. 3rd Int. Conf. Biomed. Eng.* 2007, pp. 502–505.
- [10] X. Li and M. T. Orchard, "New edge-directed interpolation," *IEEE Trans. Image Process.*, vol. 10, no. 10, pp. 1521–1527, Apr. 2001.
- [11] R. M. Slone, D. H. Foos, B. R. Whiting, E. Muka, D. A. Rubin, T. K. Pilgram, K. S. Kohm, S. S. Young, P. Ho, and D. D. Hendrickson, "Assessment of visually lossless irreversible image compression: Comparison of three methods by using an image-comparison workstation," *Radiology*, vol. 215, no. 2, pp. 543–553, May 2000.
- [12] A. Ng, "Sparse autoencoder," *Lect. Notes*, vol. 72, pp. 1–19, Jan. 2011.
- [13] V. Muralidharan, Y. Dong, and W. David Pan, "A comparison of feature selection methods for machine learning based automatic malarial cell recognition in wholeslide images," in *Proc. IEEE-EMBS Int. Conf. Biomed. Health Informat. (BHI)*, Feb. 2016, pp. 216–219.
- [14] H. Yin and N. K. Jha, "A health decision support system for disease diagnosis based on wearable medical sensors and machine learning ensembles," *IEEE Trans. Multi-Scale Comput. Syst.*, vol. 3, no. 4, pp. 228–241, Oct. 2017.
- [15] I. Arel, D. C. Rose, and T. P. Karnowski, "Deep machine learning—A new frontier in artificial intelligence research [research frontier]," *IEEE Comput. Intell. Mag.*, vol. 5, no. 4, pp. 13–18, Nov. 2010.
- [16] V. Nair and G. E. Hinton, "3D object recognition with deep belief nets," in *Proc. Adv. Neural Inf. Process. Syst.*, 2009, pp. 1339–1347.
- [17] B. P. Nigam, M. K. Sundaresan, and T.-Y. Wu, "Theory of multiple scattering: Second born approximation and corrections to Molière's work," *Phys. Rev.*, vol. 115, no. 3, pp. 491–502, Aug. 1959.
- [18] J. Schluter and C. Osendorfer, "Music similarity estimation with the mean-covariance restricted Boltzmann machine," in *Proc. 10th Int. Conf. Mach. Learn. Appl. Workshops*, Dec. 2011, pp. 469–477.
- [19] C.-Y. Liou, W.-C. Cheng, J.-W. Liou, and D.-R. Liou, "Autoencoder for words," *Neurocomputing*, vol. 139, pp. 84–96, Sep. 2014.
- [20] N. Srivastava, G. E. Hinton, A. Krizhevsky, I. Sutskever, and R. Salakhutdinov, "Dropout: A simple way to prevent neural networks from overfitting," *J. Mach. Learn. Res.*, vol. 15, no. 1, pp. 1929–1958, 2014.
- [21] G. E. Hinton, "Reducing the dimensionality of data with neural networks," *Science*, vol. 313, no. 5786, pp. 504–507, Jul. 2006.
- [22] P. Baldi and P. J. Sadowski, "Understanding dropout," in *Proc. Adv. Neural Inf. Process. Syst.*, 2013, pp. 2814–2822.
- [23] D. Warde-Farley, I. J. Goodfellow, A. Courville, and Y. Bengio, "An empirical analysis of dropout in piecewise linear networks," 2013, *arXiv:1312.6197*. [Online]. Available: <http://arxiv.org/abs/1312.6197>
- [24] C. Thompson, Kevyn, and R. Nickolov, "A clustering-based algorithm for automatic document separation," in *Proc. Workshop Inf. Retr. OCR, From Converting Content Grasping, Meaning*, Tampere, Finland, 2002, pp. 1–5.
- [25] W. C. Mann and S. A. Thompson, "Rhetorical structure theory: Toward a functional theory of text organization," *Interdiscipl. J. for Study Discourse*, vol. 8, no. 3, pp. 243–281, 1988.
- [26] D. Li, M. L. Seltzer, D. Yu, A. Acero, A. R. Mohamed, and G. Hinton, "Binary coding of speech spectrograms using a deep auto-encoder," in *Proc. 11th Annu. Conf. Int. Speech Commun. Assoc.*, 2010, pp. 1–10.
- [27] N. Hatipoglu and G. Bilgin, "Cell segmentation in histopathological images with deep learning algorithms by utilizing spatial relationships," *Med. Biol. Eng. Comput.*, vol. 55, no. 10, pp. 1829–1848, Oct. 2017.
- [28] J. Masci, U. Meier, D. Cirean, and J. Schmidhuber, "Stacked convolutional auto-encoders for hierarchical feature extraction," in *Proc. Artif. Neural Netw. Mach. Learn.*, 2011, pp. 52–59.
- [29] C. Hu, R. Ju, Y. Shen, P. Zhou, and Q. Li, "Clinical decision support for Alzheimer's disease based on deep learning and brain network," in *Proc. IEEE Int. Conf. Commun. (ICC)*, May 2016, pp. 1–6.
- [30] J. Shan and L. Li, "A deep learning method for microaneurysm detection in fundus images," in *Proc. IEEE 1st Int. Conf. Connected Health, Appl., Syst. Eng. Technol. (CHASE)*, Jun. 2016, pp. 357–358.
- [31] S. Chen, J. Qin, X. Ji, B. Lei, T. Wang, D. Ni, and J.-Z. Cheng, "Automatic scoring of multiple semantic attributes with multi-task feature leverage: A study on pulmonary nodules in CT images," *IEEE Trans. Med. Imag.*, vol. 36, no. 3, pp. 802–814, Mar. 2017.
- [32] P. Vincent, H. Larochelle, I. Lajoie, Y. Bengio, and P.-A. Manzagol, "Stacked denoising autoencoders: Learning useful representations in a deep network with a local denoising criterion," *J. Mach. Learn. Res.*, vol. 11, no. 12, pp. 3371–3408, Dec. 2010.
- [33] S. Rifai, Y. Bengio, Y. Dauphin, and P. Vincent, "A generative process for sampling contractive auto-encoders," 2012, *arXiv:1206.6434*. [Online]. Available: <http://arxiv.org/abs/1206.6434>
- [34] J. Zhang, K. Li, Y. Liang, and N. Li, "Learning 3D faces from 2D images via stacked contractive autoencoder," *Neurocomputing*, vol. 257, pp. 67–78, Sep. 2017.
- [35] E. Hosseini-Asl, J. M. Zurada, and O. Nasraoui, "Deep learning of part-based representation of data using sparse autoencoders with nonnegativity constraints," *IEEE Trans. Neural Netw. Learn. Syst.*, vol. 27, no. 12, pp. 2486–2498, Dec. 2016.
- [36] X. Shen and Y. Wu, "A unified approach to salient object detection via low rank matrix recovery," in *Proc. IEEE Conf. Comput. Vis. Pattern Recognit.*, Jun. 2012, pp. 853–860.
- [37] C. Shen and Q. Zhao, "Learning to predict eye fixations for semantic contents using multi-layer sparse network," *Neurocomputing*, vol. 138, pp. 61–68, Aug. 2014.
- [38] C. Xia, F. Qi, G. Shi, and P. Wang, "Nonlocal center-surround reconstruction-based bottom-up saliency estimation," *Pattern Recognit.*, vol. 48, no. 4, pp. 1337–1348, 2015.
- [39] A. Torralba, A. Oliva, M. S. Castelhano, and J. M. Henderson, "Contextual guidance of eye movements and attention in real-world scenes: The role of global features in object search," *Psychol. Rev.*, vol. 113, no. 4, pp. 766–786, 2006.
- [40] A. M. Treisman and G. Gelade, "A feature-integration theory of attention," *Cognit. Psychol.*, vol. 12, no. 1, pp. 97–136, 1980.
- [41] G. A. Carpenter and S. Grossberg, *Adaptive Resonance Theory*. 2017, pp. 24–40.
- [42] G. Kootstra, A. Nederveen, and B. D. Boer, "Paying attention to symmetry," in *Proc. Brit. Mach. Vis. Conf.*, 2008, pp. 1115–1125.

- [43] H. J. Seo and P. Milanfar, "Static and space-time visual saliency detection by self-resemblance," *J. Vis.*, vol. 9, no. 12, p. 15, Nov. 2009.
- [44] R. Zhao, W. Ouyang, and X. Wang, "Unsupervised salience learning for person re-identification," in *Proc. IEEE Conf. Comput. Vis. Pattern Recognit.*, Jun. 2013, pp. 3586–3593.
- [45] J. Han, D. Zhang, X. Hu, L. Guo, J. Ren, and F. Wu, "Background prior-based salient object detection via deep reconstruction residual," *IEEE Trans. Circuits Syst. Video Technol.*, vol. 25, no. 8, pp. 1309–1321, Aug. 2015.
- [46] K. Simonyan, A. Vedaldi, and A. Zisserman, "Deep inside convolutional networks: Visualising image classification models and saliency maps," 2013, *arXiv:1312.6034*. [Online]. Available: <http://arxiv.org/abs/1312.6034>
- [47] B. Taille and M. G. Ortiz, "Separating inference from feature learning in deep unsupervised visual saliency estimation," in *Proc. Int. Joint Conf. Neural Netw. (IJCNN)*, May 2017, pp. 1195–1201.
- [48] Q. Zhao and C. Koch, "Learning visual saliency by combining feature maps in a nonlinear manner using AdaBoost," *J. Vis.*, vol. 12, no. 6, p. 22, Jun. 2012.
- [49] G. S. Babu, P. Zhao, and X. L. Li, "Deep convolutional neural network based regression approach for estimation of remaining useful life," in *Proc. Int. Conf. Database Syst. Adv. Appl.*, 2016, pp. 214–228.
- [50] G. Li and Y. Yu, "Visual saliency based on multiscale deep features," in *Proc. IEEE Conf. Comput. Vis. Pattern Recognit. (CVPR)*, Jun. 2015, pp. 5455–5463.
- [51] K. Sun, J. Zhang, C. Zhang, and J. Hu, "Generalized extreme learning machine autoencoder and a new deep neural network," *Neurocomputing*, vol. 230, pp. 374–381, Mar. 2017.
- [52] R. Miotto, F. Wang, S. Wang, X. Jiang, and J. T. Dudley, "Deep learning for healthcare: Review, opportunities and challenges," *Briefings Bioinf.*, vol. 19, no. 6, pp. 1236–1246, Nov. 2018.
- [53] J. C. Patra and A. C. Kot, "Nonlinear dynamic system identification using chebyshev functional link artificial neural networks," *IEEE Trans. Syst., Man, Cybern. B. Cybern.*, vol. 32, no. 4, pp. 505–511, Aug. 2002.
- [54] J. Xu, L. Xiang, Q. Liu, H. Gilmore, J. Wu, J. Tang, and A. Madabhushi, "Stacked sparse autoencoder (SSAE) for nuclei detection on breast cancer histopathology images," *IEEE Trans. Med. Imag.*, vol. 35, no. 1, pp. 119–130, Jan. 2016.
- [55] P. P. K. Chan, Z. Lin, X. Hu, E. C. C. Tsang, and D. S. Yeung, "Sensitivity based robust learning for stacked autoencoder against evasion attack," *Neurocomputing*, vol. 267, pp. 572–580, Dec. 2017.
- [56] C. Roa, A. Alfonso, J. E. Arevalo Ovalle, A. Madabhushi, and F. A. G. Osorio, "A deep learning architecture for image representation, visual interpretability and automated basal-cell carcinoma cancer detection," in *Proc. Int. Conf. Med. Image Comput. Comput.-Assist. Intervent.*, 2013, pp. 403–410.
- [57] M. Woźniak, D. Poáap, L. Koámider, and T. Cäapa, "Automated fluorescence microscopy image analysis of pseudomonas aeruginosa bacteria in alive and dead stadium," *Eng. Appl. Artif. Intell.*, vol. 67, pp. 100–110, Jan. 2018.
- [58] D. Polap and M. Wozniak, "Bacteria shape classification by the use of region covariance and convolutional neural network," in *Proc. Int. Joint Conf. Neural Netw. (IJCNN)*, Jul. 2019, pp. 1–7.
- [59] J. A. Quinn, R. Nakasi, P. K. B. Mugagga, P. Byanyima, W. Lubega, and A. Andama, "Deep convolutional neural networks for microscopy-based point of care diagnostics," in *Proc. Mach. Learn. Healthcare Conf.*, 2016, pp. 271–281.
- [60] G. Litjens, T. Kooi, B. Ehteshami Bejnordi, A. Arindra Adiyoso Setio, F. Ciompi, M. Ghafoorian, J. A. W. M. van der Laak, B. van Ginneken, and C. I. Sánchez, "A survey on deep learning in medical image analysis," 2017, *arXiv:1702.05747*. [Online]. Available: <http://arxiv.org/abs/1702.05747>
- [61] D. Bibin, M. S. Nair, and P. Punitha, "Malaria parasite detection from peripheral blood smear images using deep belief networks," *IEEE Access*, vol. 5, pp. 9099–9108, 2017.
- [62] H.-C. Shin, H. R. Roth, M. Gao, L. Lu, Z. Xu, I. Nogues, J. Yao, D. Mollura, and R. M. Summers, "Deep convolutional neural networks for computer-aided detection: CNN architectures, dataset characteristics and transfer learning," *IEEE Trans. Med. Imag.*, vol. 35, no. 5, pp. 1285–1298, May 2016.



PRIYADARSHINI ADYASHA PATTANAIK

received the Ph.D. degree in computer science and engineering. Her areas of expertise are medical image analysis and visualization, machine learning (deep learning), computer vision, and the Internet of Things. Her research interests include developing machine learning algorithms with deep neural networks and graphical models for visual computing, including medical image analysis and disease detection. Collaborations further supplement her experience in international research projects involving research stay for her Postdoctoral fellowship at Telecom SudParis (Public), France.



MOHIT MITTAL (Member, IEEE)

received the B.Tech. and M.Tech. degrees in computer science and engineering from Guru Nanak Dev University, Amritsar, in 2010 and 2011 respectively, and the Ph.D. degree from Gurukula Kangri Vishwavidyalaya, Uttarakhand, India, 2018. He is a Postdoctoral Researcher at the Department of Information Science and Technology, Kyoto Sangyo University, Kyoto, Japan. He has published more than 35 research articles in various international journals and conferences. His research interests include wireless sensor networks, artificial intelligence, NLP, data mining, and machine learning.



MOHAMMAD ZUBAIR KHAN

received the Ph.D. degree in computer science and information technology from the Faculty of Engineering, M. J. P. Rohilkhand University, Bareilly, India, and the M.Tech. degree in computer science and engineering from U. P. Technical University, Lucknow, India, in 2006. He is currently working as an Associate Professor with the Department of Computer Science, College of Computer Science and Engineering, Taibah University. He has worked

as the Head and an Associate Professor with the Department of Computer Science and Engineering, Invertis University, Bareilly. He has published more than 40 journal articles and conference papers. He has more than 15 years teaching and research experience. His current research interests include data mining, machine learning, parallel and distributed computing, and computer networks. He has been a member of the Computer Society of India, since 2004.

...